Design, conception, and assessment of an innovative liquid distributor for separation column

Sergio da Cunha, Baptiste Dejean, Benoit Mizzi, David Rouzineau, Michel Meyer, Vincent Gerbaud, Nataliya Shcherbakova

Design, Conception, and Assessment of an Innovative Liquid Distributor for Separation Column

Sergio da Cunha, Baptiste Dejean, Benoit Mizzi, Nataliya Shcherbakova, David Rouzineau*, Michel Meyer, Vincent Gerbaud

Laboratoire de Génie Chimique, Université de Toulouse, CNRS, INP, UPS, Toulouse, France

* corresponding author: david.rouzineau@ensiacet.fr

Abstract

Liquid distributor is an important internal in packed distillation columns. One of the key features of this equipment is the drip point density, which corresponds to the number of irrigation points per area of the cross-section. For gravity liquid distributors, increasing the number of irrigation holes generally requires small hole diameters, which makes the equipment more sensitive to plugging. In this work, we disclose a new gravity liquid distributor that achieves large drip point densities without requiring smaller irrigation holes. This distributor is an adaptation of the classic orifice-pan type, in which we add a tree-like structure made of wires to spread the liquid dripping from the orifices. The liquid flows outside the wires and splits several times over the different branching levels before falling on the packed bed. From an orifice-pan configuration with drip point density of 736 pts/m^2, we designed and constructed enhanced distributors with a theoretical irrigation density of 14,800 pts/m2. Performance comparison using a recently disclosed structured packing shows that these enhanced distributors can decrease HETP from 0.45m to 0.27m.

Nomenclature

Symbols

A, B, C	area ratios used to calculate the quality rating index
A_g	packing's specific surface area (m^2/m^3)
D_Q	quality rating index
d_w	wire diameter (mm)
d^*	dimensionless wire diameter
g	gravity (m/s^2)
l_w	wire length (mm)
l_c	capillary length (mm)
M_f	maldistribution factor
N	number of regions the cross section is divided to calculate the maldistribution factor
N_l	number of layers on a distributor
Q	volumetric liquid flowrate (m^3/s)
r_c	spline's radius of curvature (mm)
We	Weber number
θ	angle between a wire and the vertical axis (º)
ρ	liquid density (kg/m^3)
γ	surface tension (N/m)
ϵ	packing's void fraction

Abbreviations

D1, D2, D3	tree-like distributors used in experiments
HETP	height equivalent of a theoretical plate
S_{BL}	liquid sample from the bottom of the column
S_{TL}	liquid sample from the top of the column
TS	tetra spline

1. Introduction

Liquid distributors and redistributors are critical components in packed distillation columns. In this work, aiming at reducing maldistribution, we disclose a new gravity liquid distributor that achieves large drip point densities without requiring smaller irrigation holes. The design parameters of the tree like wire architecture, namely wire diameter and length, angles and number of layers, are carefully selected to enable liquid wetting flow on the wire outside, avoiding excess pressure drop. Liquid distributors are used to ensure an even distribution of liquid throughout the cross-section of the column. Ideally, this equipment should provide a large number of evenly distributed irrigation points and a large area for upward countercurrent vapor flow. Further, their design should aim for large turndown ratios to give room for operational fluctuations and changes in nominal flow rates (due to increase/decrease in demand, for example). However, these requirements are often conflicting in practice, and different types of distributors are available in the market according to the designer's priority.

Distributors are usually divided in two categories, according to the driving force for the liquid flow within: pressure or gravity. The most classic example of pressure distributors is the perforated pipe (Kister, 1990; Kister et al., 2008). It consists of several perforated pipes branching out from a main tube. The liquid stream is pumped through the main tube, where it splits into different streams as the liquid flows along the branches. Discharge takes place through the holes on the underside of the branching pipes. This device provides a large area for upward vapor flow. However, the high liquid pressure drop induces either smaller number of holes or smaller size of holes, decreasing quality of distribution or making it prone to plugging.

Gravity distributors allow for smaller liquid pressure drops, though they generally provide smaller areas for the upward vapor flow. The driving force for liquid discharge is the weight of the liquid head built up on the distributor. Some gravity distributors, such as orifice-pan and orifice tunnel types (Kister, 1990; Kister et al., 2008), can be used as self-collecting redistributors. For this application, a hat needs to be installed on the top of the vapor risers to prevent the liquid from flowing through them. The gravity distributors aforementioned direct the vapor flow through risers and discharge the liquid through holes on the base plate. As an alternative, instead of directing the vapor stream, trough distributors (Kister, 1990; Kister et al., 2008) direct the liquid stream to troughs in which the liquid heads are built up. Vapor

flows through the gaps between the troughs, and the area available for this flow is generally higher compared to orifice-pan and orifice tunnel distributors.

The distributors discussed so far are well-established in the chemical industry and have been operated for decades, but there is still room for improvements. Recently, Eck and Kirsten (2019) proposed a new design for self-collecting liquid redistributors, with the addition of a droplet dumping tray just above the redistributor tray. Usually, when droplets fall from the bottom of a packed bed directly onto the liquid layer formed on the redistributor tray below, foam can be formed. The inventors claim that adding the so-called droplet dumping tray just above this liquid layer helps prevent foam formation. On their own, Franz and Geipel (2019) improved on classic nozzle distributors by using flat-jet nozzles and adding a drain element to them. In one of the configurations listed by the inventors, guide plates intercept liquid from the end of the flat jets at small angles. The liquid then drops from the edge of the plate. Such a drain element also protects the liquid against the rising vapor flow, and a significant reduction in entrainment can be achieved. Otherwise, the Super X-Pack distributor was designed by Nagaoka International Corporation (Manteufel, 2000; Manteufel and Koch, 2001). Like our design, it consists of interconnected wires which are fed from the distributor plates through narrow tubes enclosing the wire bundles. This is different from our invention, in which the wires split into branches in order to distribute the liquid.

The inventions above deal with relevant issues in distillation operation, namely entrainment and foaming. Yet another issue that can cause malfunction in packed columns is maldistribution. Liquid maldistribution is associated with a reduction in packing efficiency, which translates into HETP increasing by a factor as high as 3 in some cases (Kister et al., 2008). This issue makes quality of the liquid distribution one of the most relevant performance indicators for distributors. In this context, Moore and Rukovena have proposed in 1987 the distribution quality rating index (D_Q), defined as follows (Kister, 1990; Moore and Rukovena, 1987):

$$D_Q = 0.4 \times (1 - A) + 0.6B - 0.33 \times (C - 0.075) \quad \#(1)$$

This approach considers the irrigation points as drip circles whose areas are proportional to the liquid flowrate through them. Further, the sum of circle areas equals the cross-section area of the column. Parameter *A* is the fraction of the column's cross-section that is not covered by drip circles. To evaluate *B*, one needs to partition the column's cross section in 12 sectors with the same area. Sectors can be ring-like or trapezoid-like (Hanusch et al., 2019). The

smallest ratio of total circle area in a sector to this sector's area (B_1) and the smallest ratio of a sector area to its total circle area (B_2) are calculated. *B* is defined as the minimum between B_1 and B_2. Finally, *C* is the ratio of the circles' overlap area to the cross-section area of the column. The geometric representation of parameters *A*, *B* and *C* is illustrated in Hanusch et al. (2019) and in Kister (1990). Typical values of index D_Q are 0.1 to 0.7 (Kister et al., 2008).

Another index commonly used to evaluate quality of liquid distribution is the maldistribution factor M_f (Hoek et al., 1986; Marcandelli et al., 2000). This index is similar to a coefficient of variation, measuring the deviation from a perfectly homogeneous distribution. To calculate this index, one needs to divide the column's cross-section into *N* regions of equal area. Later on, M_f can be calculated by measuring the liquid flow across each of these *N* regions:

$$M_f = \sqrt{\frac{1}{N(N-1)} \sum_i \left(\frac{Q_i - Q_{mean}}{Q_{mean}} \right)^2} \quad \#(2)$$

In Eq. 2, Q_i is the liquid flowrate across region *i*, and Q_{mean} is the average flowrate over the *N* regions. M_f varies between 0 and 1. A value of 0 indicates a perfectly homogeneous distribution, whereas 1 corresponds to the case where all the liquid flows through only one region.

In the present manuscript, we report a solution to maldistribution that consists in increasing the number of irrigation points without increasing the number of holes on the distributor's plate. This can be achieved by incorporating an innovative tree-like structure (Rouzineau et al., 2020) that guides the liquid dripping from each hole and separates it into several branches.

The rest of the paper is organized as follows. Section 2 overviews the novel distributor concept and reviews several features developed by our team that will be useful for distributor design. First we recall the characterization of liquid flow on a wire and along tetrasplines, according to the experimental results shown in Dejean et al. (2020). We also review design and performance of a new type of packing, called Tetra Spline (TS) packing (Kawas et al., 2021), which is used in the test rigs described by the end of Section 2. Section 3 discusses criteria for choosing distributor design and it details three configurations chosen according to these criteria. Their performance is assessed and later compared with Sulzer's perforated pipe and regular orifice-pan distributors. Finally, Section 4 reviews the main findings of this work.

2. Materials and Methods

2.1 Tree-like liquid distributor overview

In general, distributor's performance increases with respect to the number of irrigation points. However, designing a liquid distributor with a high number of holes could make it prone to plugging or increase pressure drop, as the diameter of the holes would have to be smaller. The solution proposed here is to increase the number of irrigation points without increasing the number of holes on the distributor's plate. This can be achieved by incorporating a tree-like structure that guides the liquid dripping from each hole and separates it into several branches.

Constructal theory claims that, in general, tree-structures are the best architecture to realize point-to-area flow (Bejan and Lorente, 2004). So far, the liquid distributors developed using this theory have had fluid flowing inside the structure, as in the case of vascular networks developed for self-healing materials (Cho et al., 2010). Such a network is unsuitable for distillation applications because it would result in large liquid heads, due to the friction inside the tubes. The workaround is to conceive a tree distributor with the liquid flowing outside the branches. That is the key innovation in the invention disclosed by Rouzineau et al. (2020).

In the arrangement proposed by the inventors, the liquid does not drip directly from the distributor plate holes to the packed bed below. Instead, it flows along the outer surface of wires, driven by gravity. Each wire later splits into 3 different branches, spreading the irrigation along the column's cross-section. Wires are shaped as splines instead of a straight form, to ensure a smooth transition between different branching levels (Dejean et al., 2020) that prevents exaggerated liquid bead formation at level junctions. Further, wire diameter is allowed to vary along the tree-structure levels. Figure 1 shows an example of a liquid distributor that we have designed according to such criteria. The distributor displayed in Figure 1 and the others used in this work were designed using Autodesk Inventor software (Autodesk, 2019).

The distributor depicted in Figure 1a distributes the liquid from 13 primary irrigation points. On the underside of the plate one can see the spaces between the holes and the vertical wires, through which the liquid flows. Figure 1b shows the orifice-pan structure on the top of the distributor. There are 12 chimneys for the upward vapor flow. Only the 3 at the center are covered by a hat, as in our experiments the liquid falling from above is mostly concentrated in the center of the column. However, hats can be added to the top of the other chimneys if

necessary. Figure 1c depicts the bottom view of the distributor. There are 262 potential irrigation points, which can be divided in 13 triangular sectors (one per plate hole). These triangles are actually the bases of pyramid-like structures similar to the one shown in Figure 1d. The pyramid in Figure 1d exhibits 6 branching levels. Dimensions of the 3 tree-like distributors studied in this paper will be detailed later in Table 2.

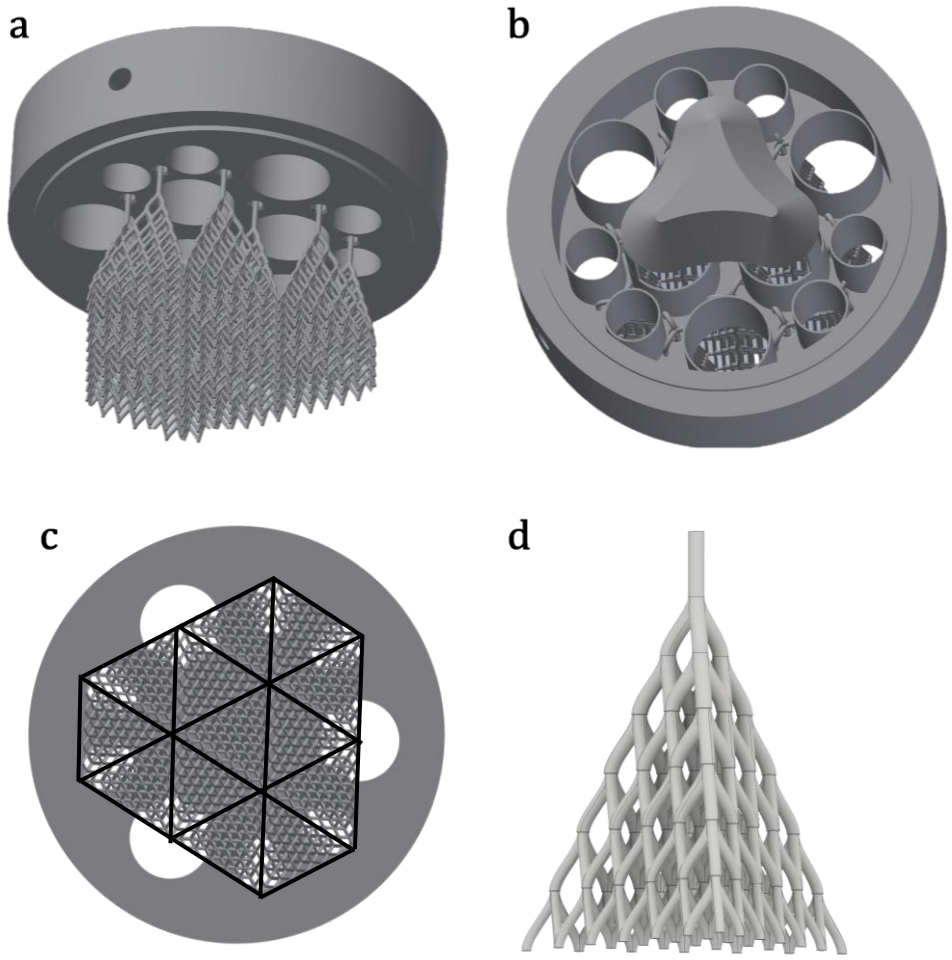

Figure 1 – (a) isometric, (b) top and (c) bottom views of a tree-structured liquid distributor; (d) pyramid distributing liquid from a single hole on the distributor plate

It would be naive to assume that all the wires in the structure shown in Figure 1a are wet during column's operation. Indeed, experimental results for liquid flow down a tetraspline wire structure suggest that the stream sometimes splits over 2 out of the 3 children branches (Dejean et al., 2020). However, the number of redundancies over the different branching levels helps preventing large dry areas. Redundancies refer to the reconnections happening along the several branching levels. They ensure that the offspring (children, grandchildren, …) of a dry wire can still be wet, as there are other paths for the liquid to reach these wires.

Finally, it is worth noting that a somewhat similar structure has been employed by Nagaoka International Corporation to conceive a new packing for distillation columns, called Super X-Pack (Manteufel, 2000; Manteufel and Koch, 2001). This packing also consists of wires, which are interconnected either in a triangular matrix or in a square matrix. All the threads of the packing are regrouped in wire bundles at the head of the package, and the liquid leaves the distributor plates through narrow tubes enclosing these bundles. The wire bundles, which are initially confined in these tubes and very close to each other, spread once they leave the tubes and eventually connect to the regular packing structure. This is different from our invention, in which the wires split into branches in order to distribute the liquid.

2.2 Characterization of flow along tetrahedron edges

Dejean et al. (2020) made several experiments on the flow of liquid films along the surface of vertical wires and against an uprising gas flow. In their experimental setup, liquid inlet flow is controlled by a syringe pump. A connector controls the injection diameter, and the liquid film thickness on the wire (δ) is measured using a high velocity camera. Wire length is kept below 20mm to avoid instabilities, and the upward gas flow is controlled using a needle valve and a flowmeter. Gas (air) is first humidified in a different chamber, in order to avoid evaporation of the liquid on the wire. Moreover, gas flowrates are set so that the corresponding F-factors in the wire chamber do not exceed 3 $Pa^{0.5}$. We recall that F-factor is given by the product of the vapor superficial velocity times the square root of the vapor density, and that high F-factors are associated to flooding. One of the key results obtained by Dejean et al. (2020) is that the type of liquid being used in the experiments affects the flow regime. For water, flow regime shifts from partial wetting (with the presence of liquid beads) to full wetting (without beads) for liquid flowrates above around 20 mL/min. For ethanol, full wetting regime is obtained even for liquid flowrates as low as 5 mL/min.

Dejean et al. (2020) also studied liquid flow along a tetrahedron structure made of wires, which resembles the repeating pattern of the Tetra Spline (TS) structured packing disclosed in Kawas et al. (2021). This motif consists of a vertical wire that splits into 3 inclined branches. These branches are straight wires of common length l_w, circular cross-sections of diameter d_w, and inclination θ with respect to the vertical wire. Three different liquids were used for experiments: demineralized water, ethanol and a 50-50 ethanol-water mixture. The setup for experiments is similar to the one used in the study of liquid films along the surface of vertical wires, but the single wire is replaced by the tetrahedron element. Besides, instead of

measuring δ, Dejean et al. (2020) were more interested in the different flow regimes taking place when studying the structure. Three main regimes have been observed: capillary, inertial and wetting. Capillary flow takes place when surface tension dominates over other forces. This regime is characterized by the formation of droplet streams, and liquid flows only on 1 of the 3 edges. Inertial flow is observed when inertia controls the flow, rendering surface tension negligeable. In this state, the wires are not capable of changing flow direction. Wetting is achieved when inertia and surface tension are of the same order of magnitude. In this case, the flow is smoothly repartitioned over 2 or 3 edges. Furthermore, two intermediate zones were observed. One of them is characterized by surface tension forces slightly stronger than inertial forces, and it corresponds to a flow that is unevenly partitioned over the tetrahedron branches. The second intermediate zone is obtained when inertial forces are slightly stronger; in this case, the three wires are wetted, but a liquid membrane englobes two of them.

Generally, high flowrates and low wire diameters favor inertial regime, whereas low flowrates and low wire diameters favor capillary flow. Wire length does not play a significant role on the flow regime, though it was observed that for l_w < 10mm the liquid flow englobes the entire structure instead of splitting over the edges. Similarly, for $\theta < 30°$ separation of the liquid stream cannot be achieved. Further, for $\theta > 40°$ the liquid stream detaches from the wires.

The remaining parameters studied by the authors were gas countercurrent flowrate and liquid type. It was found that gas countercurrent does not affect flow regime along the tetrahedron for F-factors smaller than 3 $Pa^{0.5}$. Liquid type however has a major impact on the flow. Wetting flow can be obtained for some ethanol flowrates at relatively small wire diameters. The minimum wire diameter required to achieve the wetting regime is higher for the 50-50 ethanol-water mixture. Finally, wetting could not be observed for the experiments using pure water, likely because the wire diameters were not large enough.

Based on these experiments, Dejean et al. (2020) established a mapping relating the flow regimes over the tetrahedron to the dimensionless liquid flowrate (Weber number, We) and wire diameter (d^*). These dimensionless quantities are defined in Eqs. 3, 4.

$$We = \frac{\rho Q}{\gamma d_w^3} \quad \#(3)$$

$$d^* = \frac{d_w}{l_c} \quad \#(4)$$

In Eqs. 3, 4, ρ is the liquid density, Q is volumetric flowrate, γ is the surface tension and l_c is the capillary length, defined as follows:

$$l_c = \sqrt{\gamma/\rho g} \quad \#(5)$$

According to the flow regime cartography obtained by the authors, the wetting region corresponds to d* and We in the following range:

$$d^* \geq 1.3 \quad \#(6)$$

$$10^{-0.815(d^*-1.3)} \leq We \leq 10^{1.429(d^*-1.3)} \#(7)$$

The practical consequence of Eq. 7 is limiting the number of layers in the tree-like distributor. Indeed, the flow per wire decreases in the structure shown in Figure 1d as the number of layers increases. This can result in *We* values far below the minimum limit in Eq. 7, giving rise capillarity effects that prevent further distribution.

2.3 Tetra Spline packing

One of the packings used in the experiments to evaluate the performance of the novel liquid distributor was the Tetra Spline (TS) packing (Kawas et al., 2021). This packing consists of a wire structure replicating a tetrahedron pattern, with the mixture flowing outside the wires. The liquid is expected to flow along the surface of these wires, improving distribution and providing a large contact area for mass and heat exchange. Different from the tetrahedron unit mentioned in Section 2.2, the wires are shaped as splines in this packing to improve liquid repartition. Further, the layers alternate between regular and unregular tetrahedrons in order to prevent gas chimneys in the packing. The packed beds were fabricated via 3D-printing, using either polyamide or stainless steel as material. These two latter features, namely the alternating tetrahedron pattern and the fabrication via additive manufacturing, are the key differences between the TS packing and the Super X-pack mentioned in Section 2.1.

HETP experiments with TS packing were conducted by Kawas et al. (2021) using wire diameters (d_w) in the range 0.5mm – 2.75mm, and specific surface area (A_g) in the range 139m^2/m^3 – 387m^2/m^3. Mellapak 250Y was used as reference packing for comparison.

Packing material was found to influence the efficiency of the column only for smaller diameters. At $d_w = 1.5$mm, the stainless steel packing showed ~10% decrease in HETP compared to the polyamide packing. At $d_w = 2.25$mm, no significant difference was observed. Further, Kawas et al. (2021) found that larger wire diameters and specific surface

areas result in lower HETP. The former is consistent with previous results (Dejean et al., 2020) showing an improvement in liquid distribution over the tetrahedron mentioned in Section 2.2 when wire diameter is increased. The low HETP values obtained for high specific surface area are clearly due to the increase in mass/heat exchange area.

Overall, the packing efficiency of TS was found comparable to that of Mellapak 250Y. Many of the TS configurations performed better than the reference packing at low vapor flowrates (F-factor < 1 Pa$^{0.5}$). Three of them outperformed Mellapak 250Y for all the vapor flowrates used in experiments, which correspond to F-factors between 0 and 2.5 Pa$^{0.5}$. The values of d_w (mm), void fraction (ϵ) and A_g (m^2/m^3) for these best configurations were: (1.5, 0.89, 281); (2.25, 0.89, 182); (1.5; 0.92, 205). The two first configurations were printed using polyamide, whereas the third was printed using stainless steel.

In the present work, HETP experiments were performed with a TS packed bed made of polyamide. Its configuration is characterized by $d_w = 1.5$mm, void fraction of 0.92 and a specific area of 205m^2/m^3. Further, the wire lengths were fixed at $l_w = 12$mm, and the inclinations of the wires with respect to the vertical were $\theta_1 = 30°$ and $\theta_2 = 40°$ respectively for the regular and unregular tetrahedron layers.

2.4 Characterization of liquid distributor

Liquid distributor performance can be evaluated either via the quality of the liquid distribution it provides, or directly through its impact on the HEPT value of a standard distillation column. The corresponding experimental setups are described in Sections 2.4.1 and 2.4.2, respectively.

2.4.1 Assessment of liquid distribution

Liquid distribution is assessed using the maldistribution factor M_f discussed in Section 1, and the test rig used for experiments is shown in Figure 2. The column shell is made of glass, with inner diameter of 150mm. As depicted in the figure, liquid is pumped (1) to the top of the column, using a flowmeter (2) to regulate the flow. The inlet stream is distributed over the cross-section by a liquid distributor (3). The outlet then falls onto a liquid collector (5), which is divided in 21 zones with the same area. Each zone has an orifice with a tube (6) attached to it, and the flow exiting through each of these tubes is measured using a flowmeter (FHK-LCD Digmesa). In some experiments, 1 m of the TS packing described in Section 2.3 (4) was added between the liquid distributor and the collector, to study the effect of initial distribution on the distribution obtained from the packing.

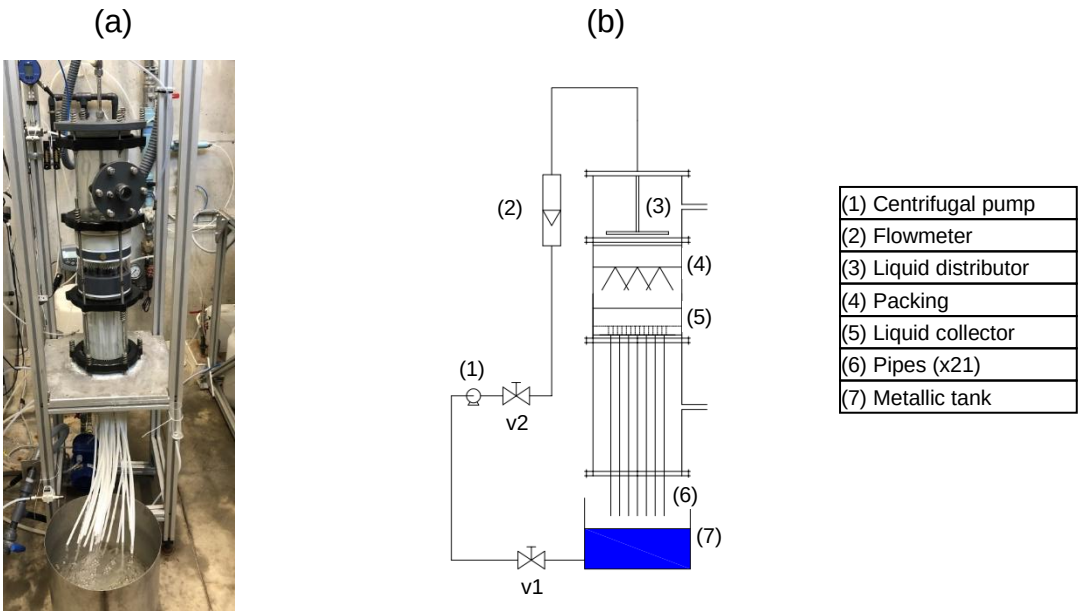

Figure 2 – Picture (a) and sketch (b) of the experimental setup measuring M_f for different distributors

The liquid collector used for experiments is similar to the one used by Lämmermann et al. (2016), and it is depicted later in Figure 6b. It was designed using Autodesk Inventor (2019), and fabricated by extrusion. The diameter of its outlet holes is 6 mm.

The setup for experiments was validated using an orifice-pan distributor with 13 holes, and a perforated pipe distributor provided by Sulzer with 5 drip points. The hole diameter is 2.7mm for the orifice-pan distributor, and its design is very similar to the one in Figure 1b. For Sulzer's perforated pipe distributor, diameter is 3.2mm for the central hole and 5.2mm for the remaining 4 holes. The theoretical M_f values for perforated pipe and orifice-pan distributors are respectively 0.421 and 0.236. The values obtained with the experimental setup shown in Figure 2 were 0.404 and 0.218, and remained unchanged with respect to liquid flowrate, which validates the test rig. The small difference between the theoretical and the experimental values is probably due to the interval of accuracy in diameter and liquid flowrate measurements.

After validation, we tested 3 different tree-like distributor configurations (D1, D2, D3). Details for these configurations are shown later in Table 2 and Figure 4. Finally, most of the measurements used pure water as the flowing substance. Only some additional experiments with distributor D3 used mixtures of ethanol (3.1 wt% and 20.5 wt%) + water. The liquid

flowrates used in these experiments varied between 300 L/h (17 $m^3/m^2/h$) and 500 L/h (28.3 $m^3/m^2/h$).

2.4.2 Assessment of HETP

Fractionation Research, Inc. and Separation Research Program suggest standardized methods to measure the HETP in packed columns. Measurements are preferably made when operating a column at total reflux to separate a binary mixture. Samples from column's top and bottom liquid streams are taken, and their composition is used to calculate the number of theoretical plates. This calculation uses an iterative procedure where theoretical liquid composition for each stage (from top to bottom) is calculated via vapor-liquid equilibrium equations. Corresponding theoretical vapor compositions are determined by mass balance. The method uses the stream composition measured at the top of the column as the starting point. It then iterates from top to bottom until light key theoretical molar fraction becomes smaller than the molar fraction measured at the bottom. More details are available in Bessou et al. (2010).

In this work, experiments with different liquid distributors were conducted, using a packed distillation column to separate 35kg of a mixture of cyclohexane (25 wt%) + heptane. This binary mixture is recommended by Fractionation Research Inc., and it has been previously used in the literature (Olujić et al., 2000; Subawalla et al., 1997). Since the C6/C7 volatility strongly depends on composition, HETP assessment using this mixture will depend on the composition, this does not affect the comparison of our HETP measurement since we use the same total reflux, same C6/C7 feed and same bed height. However, caution should be exerted when comparing our HETP values to values published by other researchers. The setup is shown in Figure 3. A packed bed of 1 m height is placed in the column, just below the liquid distributor. Three different packings were used in the experiments: Mellapak 250Y, Pall Rings (15mm size) and the TS packing described in Section 2.3.

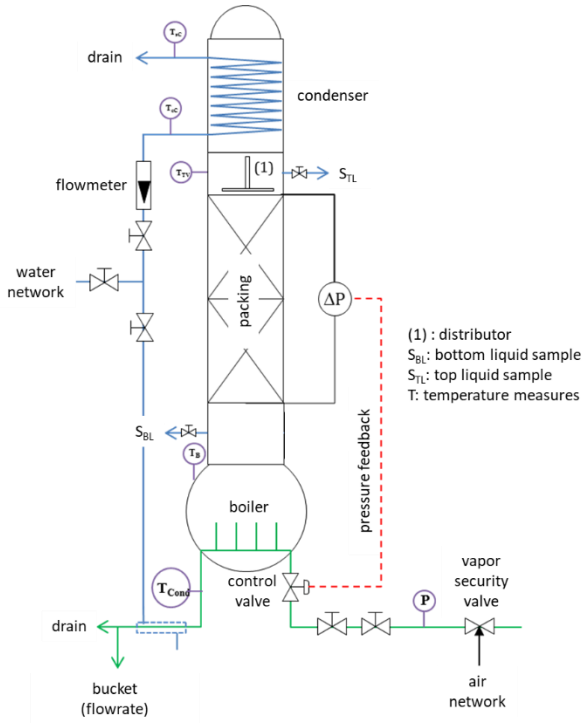

Figure 3 – Experimental setup measuring separation efficiency for different distributors. Reproduced with permission from Kawas et al. (2021).

This column operates at total reflux. Initially, a mixture of cyclohexane and heptane is placed in the thermosyphon reboiler. Reboiler duty (1-23 kW) is set by adjusting steam flowrate. As shown in Figure 3, pressure drop is measured between the top and the bottom of the packings in order to manage the control valve (heat duty) via a pressure feedback and achieve a steady state. At the top, the condenser chosen for the experiment was a coil glass condenser, using cooling water at room temperature.

Liquid samples are taken from the top (S_{TL}) and the bottom (S_{BL}) of the column every 20 minutes. A capillary tube is placed on the bottom of the liquid distributor to ensure that only liquid is taken for the S_{TL} (without any traces of gas). For the S_{BL} liquid sample, a flange-gutter system is installed just below the packed bed. Steady state is considered to be achieved when three consecutive liquid samples have identical compositions. These compositions are measured via densitometry analysis, and they are later used to calculate HETP using the method described in Bessou et al. (2010). The proposed method does not use the Fenske equation and avoids the constant volatility assumption that is sometimes assumed (Olujić et al., 2003). The selected thermodynamic model is the Wilson equation, with binary parameters $A_{ij} = 101.6831$ and $A_{ji} = -41.6534$ (Komori and Ohe, 1990) (i is the index for cyclohexane, j is the index for n-heptane).

For the Mellapak 250Y and Pall Rings packings, we tested all five distributors (orifice-pan, Sulzer's perforated pipe distributor, and the tree-like distributor configurations D1, D2 and D3). The TS packing was only tested with Sulzer's perforated pipe distributor, the orifice-pan distributor and tree-like distributor configuration D1.

3. Results and discussion

3.1 Theoretical considerations for the design of tree-like liquid distributors

Designing a distributor with a tree-like structure such as the one shown in Figure 1 requires careful analysis. The first step in the analysis is to define whether a new distributor will be designed from scratch, or if the tree-like structure will be used to retrofit an existing orifice distributor. In the former scenario, specifications for the top-plate depicted in Figure 1b (such as hole diameter, number of holes and chimneys, etc.) can be chosen by the designer. In the latter scenario, the existing distributor is reused, and only the wire structure in Figure 1d needs to be fabricated.

The key design variables are: number of layers (N_l), d_w (for each layer), l_w and θ. Note that, while the designer has the freedom to vary d_w with respect to the branching level, l_w and θ need to be kept constant. Indeed, if one of these 2 parameters is changed between consecutive layers, neighbor wires will no longer reconnect together as they do in Figure 1d.

Several constraints need to be accounted for in the design of a tree-shaped distributor. The first, most intuitive one is that the distributor should fit in the column. This constraint is easily incorporated in the design of plate-shaped distributors: it suffices to set a plate diameter inferior to the column's inner diameter. However, it becomes a more complicated issue when designing a tree-shaped distributor. For example: can a distributor with 13 holes, 6 layers, $d_w = 4\text{mm}$, $l_w = 10\text{mm}$ and $\theta = 30°$ fit in a column with inner diameter of 150mm? The answer depends on how the holes are distributed over the top plate.

As discussed in Section 2.1, to each hole corresponds a pyramid such as the one depicted in Figure 1d. The base of this pyramid is an equilateral triangle whose length (47.2 mm in this case) can be calculated as a function of N_l, l_w, θ and d_w of the last layer. Because there are 13 holes, we need to check whether we can fit 13 of such triangles in the column's cross-section. The website Wolfram Alpha (Wolfram|Alpha, 2020) provides the densest known packings for n equilateral triangles in a unit circle. For n = 13, the densest known packing forms the hexagon shape shown in Figure 1c, with its vertices on the contour of the circle. The length of

the equilateral triangles in this case equals $0.65 \times R$, where R is the circle's radius. This radius is 75mm for the column's cross-section considered here. And because $47.2\text{mm} < 0.65 \times R \approx 49\text{mm}$, we conclude that the distributor can fit the column if the position of the top plate holes is chosen wisely.

A second noteworthy constraint is on the maximum wire diameter. The wires are conceived extruding a circular shape along a spline. Therefore, wire's radius cannot exceed the spline's minimum radius of curvature. This radius of curvature r_c is a function of l_w and θ only. For $l_w = 10\text{mm}$ and $\theta = 40°$, $r_c = 1.83mm$; for $l_w = 20\text{mm}$ and $\theta = 30°$, $r_c = 4.83\text{mm}$.

The third geometric constraint regards the height of the distributor, defined as the distance between the base of the tree-structure and the bottom of the plate above. Its maximum height depends on the allowance in the column, so the designer is free to set this constraint accordingly. In the design of D1-D3 it was imposed that the distance should not exceed 200mm.

In addition to constraints imposed by equipment geometry, some constraints are imposed to ensure reasonable liquid distribution over the wires. Wire length is restricted to the interval $10\text{mm} \leq l_w \leq 20\text{mm}$. The lower wire length limit prevents the formation of a membrane englobing multiple wires, whereas the upper limit prevents the appearance of the instabilities mentioned in Section 2.2. Further, spline angle is constrained to $30° \leq \theta \leq 40°$. Here again, the lower limit prevents formation of liquid membranes englobing multiple wires, whereas the upper limit prevents liquid detachment from the wires (see Section 2.2).

Finally, a third performance constraint relates to the flow regime on each layer. Among the capillary, inertia and wetting flow regimes identified by Dejean et al. (2020), the distributor should be preferably designed so that all its layers experience wetting flow regime. Table 1 summarizes the main constraints to be considered during the design of a tree-like liquid distributor.

Table 1 – Summary of constraints considered for liquid distributor design

Type of constraint	Constraint	Variables implied
Geometric	Distributor has to fit in the column	N_l, l_w, θ, d_w
	Wire radius < spline's radius of curvature	l_w, θ, d_w
	Distributor height < allowance	N_l, l_w, θ
Performance	$10mm \leq l_w \leq 20mm$	l_w
	$30° \leq \theta \leq 40°$	θ
	Flow regime is preferably wetting	N_l, d_w

All the design considerations aforementioned were implemented in an Excel file, whose goal is to facilitate the design and screening of performant configurations. With the help of this design-assistant tool, we selected 3 distributor configurations (D1-D3) for experimental investigation. Figure 4 illustrates the different tree-structures selected, and the corresponding geometric features are given in Table 2.

Table 2 – Characteristics of the tree-like distributors used in experiments

	D1	D2	D3
No. of holes	13	13	13
Hole diameter (mm)	6.0	6.0	6.8
No. of branching levels (N_l)	6	6	6
d_w (mm)	[2.50, 2.50, 2.50, 2.25, 2.00, 1.75, 1.50]	[2.50, 2.50, 2.50, 2.25, 2.00, 1.75, 1.50]	[4.00, 4.00, 4.00, 4.00, 4.00, 4.00, 4.00]
l_w (mm)	12	10	10
θ (°)	30	36.2	36.2
Distributor height (mm)	71.4	64.7	64.7

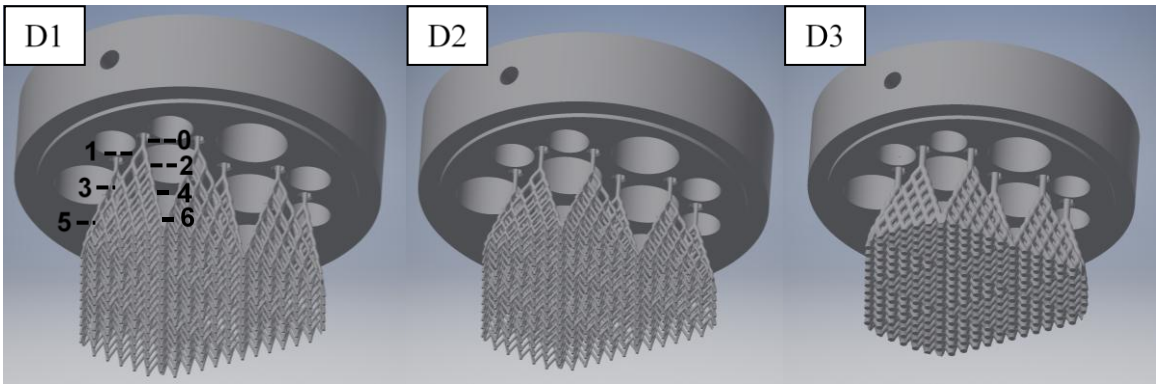

Figure 4 – Different designs of liquid distributors used in experiments

In Table 2, the number of branching levels corresponds to the number of times the distributor splits. Each level is located at a certain height, and they are numerated in Figure 4 for D1. The 0^{th} level just below the plate is the part of the distributor containing only vertical wires. Values d_w in Table 2 are the wire diameters in order from the 0^{th} to the 6^{th} layer. Finally, distributor height is measured from the bottom part of the plate until the base of the last layer.

The remaining design considerations are the drip point density and the indexes D_Q and M_f mentioned in Section 1. Distributors D1-D3 have a theoretical drip point density of ~14,800 pts/m2. This density is considerably larger than the 736 pts/m2 provided by the primary irrigation holes on the top-plate (see Figure 1b). However, close attention is necessary when comparing these values. Whereas the top plate distributes the flow evenly among its 13 holes, distribution over the 262 outlets at the base of the distributor (Figure 1c) is uneven.

Instead of focusing on the entire wire structure, let us study how a single pyramid (Figure 1d) splits the flow coming from one of the 13 holes. At the base of a 6-layer pyramid, there are in total 28 outlets. If we assume that flow is evenly partitioned over the 3 children branches of every wire, a total flow of $3^6 = 729$ would be distributed over the 28 outlets according to Figure 5.

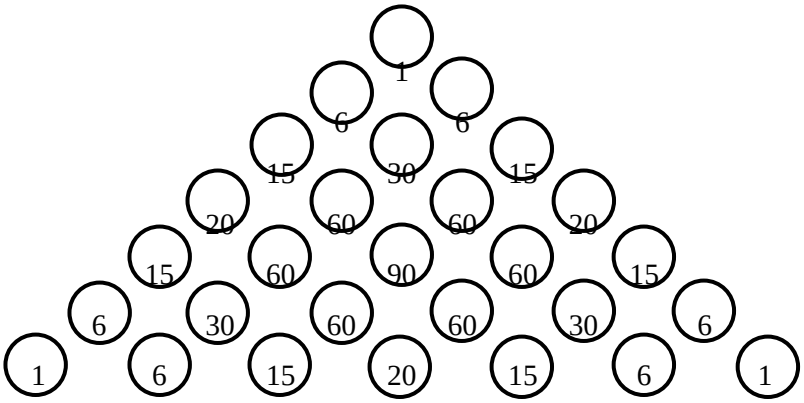

Figure 5 – Total liquid flow of 729 distributed over the 28 outlets of a 6-layer pyramid

Readers familiar with combinatorics will quickly recognize the values on the edges of the triangle shown in Figure 5 as the binomial coefficients of the 6^{th} power. A more careful analysis shows that the Pascal's triangle is retrieved if we divide each row by its lead coefficient (i.e., divide first row by 1, second row by 6, third row by 15, and so on). This pattern can be generalized for a pyramid with n layers and a flow of 3^n.

Qualitatively, Figure 5 shows that irrigation is lower near the edges and vertices of the triangles depicted in Figure 1c, growing near their barycenters. Visual observations corroborate this conclusion. However, despite this uneven distribution, we should still expect the quality of liquid distribution to be improved when the wire structure is added to the orifice-pan distributor. And we can use the data in Figure 5 to calculate the distribution quality indicators D_Q and M_f.

M_f can be obtained dividing the cross-section in 21 collection zones identical to the ones shown in Lämmermann et al. (2016) (see Figure 6). Before using experiments to measure the flowrate through each zone, we first calculate these flowrates by analyzing how the outlets are distributed over the different zones. For the simpler orifice-pan configuration with 13 holes, we consider that flow is evenly partitioned among the outlets. For the more complex tree-like structure, we use Figure 5 to estimate the outlet flow on each of the 262 dripping points. Further, because the orientation of our imaginary collection zones affects distribution of the outlet points over the zones, we average M_f values using 5 random orientations.

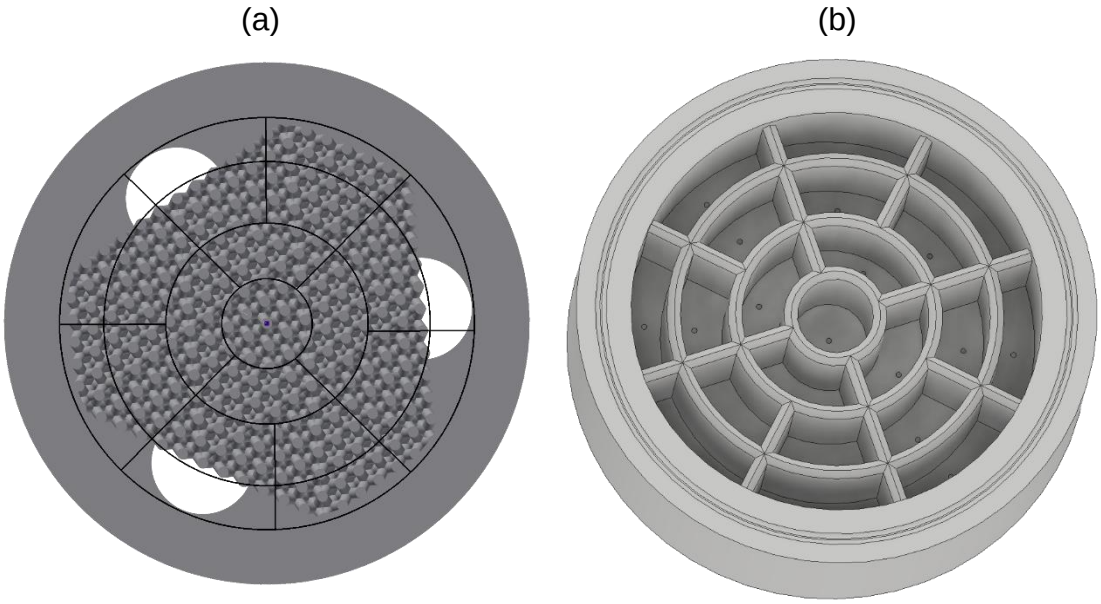

Figure 6 – (a) D3 outlets and the 21 imaginary collection zones used to calculate theoretical M_f; (b) design of the liquid collector used to measure M_f experimentally

Because D1, D2 and D3 have the same number of layers and same structure, the theoretical M_f value is the same for all of them. It varies between 0.135 and 0.137 according to collector's orientation, with an average $M_f = 0.136$. This is a significant improvement compared to $M_f = 0.236$ for the orifice-pan distributor. For comparison, Sulzer's perforated pipe distributor with 5 irrigation points has a theoretical maldistribution factor $M_f = 0.421$.

Analogously, one should expect an increase in the distribution quality index D_Q when the number of outlets is increased from 13 to 262. Nevertheless, the opposite happens: D_Q decreases from 0.40 (orifice-pan) to 0.27 (D1-D3). This is likely due to a number of inconsistencies in the D_Q method. First, the best distributor configuration predicted by Eq. 1 consists of a single outlet at the center of the cross-section, and it corresponds to $D_Q = 1.02$. Further, if instead of a single outlet we had two even outlet flows placed very close to each other and almost coincident with the center of the cross-section, the quality of the distribution should not change. Nevertheless, this new 2-outlets configuration changes D_Q to 0.06. If we arrange 3 outlets with uniform flow and close to the center of the cross-section, D_Q further decreases to -0.06. This inconsistency, which takes place when outlet points are very close to each other, is likely the reason for lower D_Q in D1-D3. Indeed, while Rukovena's distribution quality index has been successfully correlated to HETP in many industrial applications, the index does have its limitations, especially at high drip point density, like in our case, where is

behaves inconsistently as noticed by Spiegel (2006). Hence, distribution quality is assessed here using the maldistribution factor M_f instead of the more popular index D_Q.

3.2 Experimental results for liquid distribution

Experiments to measure the maldistribution factor M_f were performed according to the procedure described in Section 2.4.1. Five different types of distributors (D1, D2, D3, orifice-pan with 13 irrigation points, and Sulzer's perforated pipe distributor with 5 irrigation points) were compared for different liquid flowrates. Figure 7 shows the liquid distribution obtained from these tests at a liquid flowrate of 400 L/h (22.6 $m^3/m^2/h$).

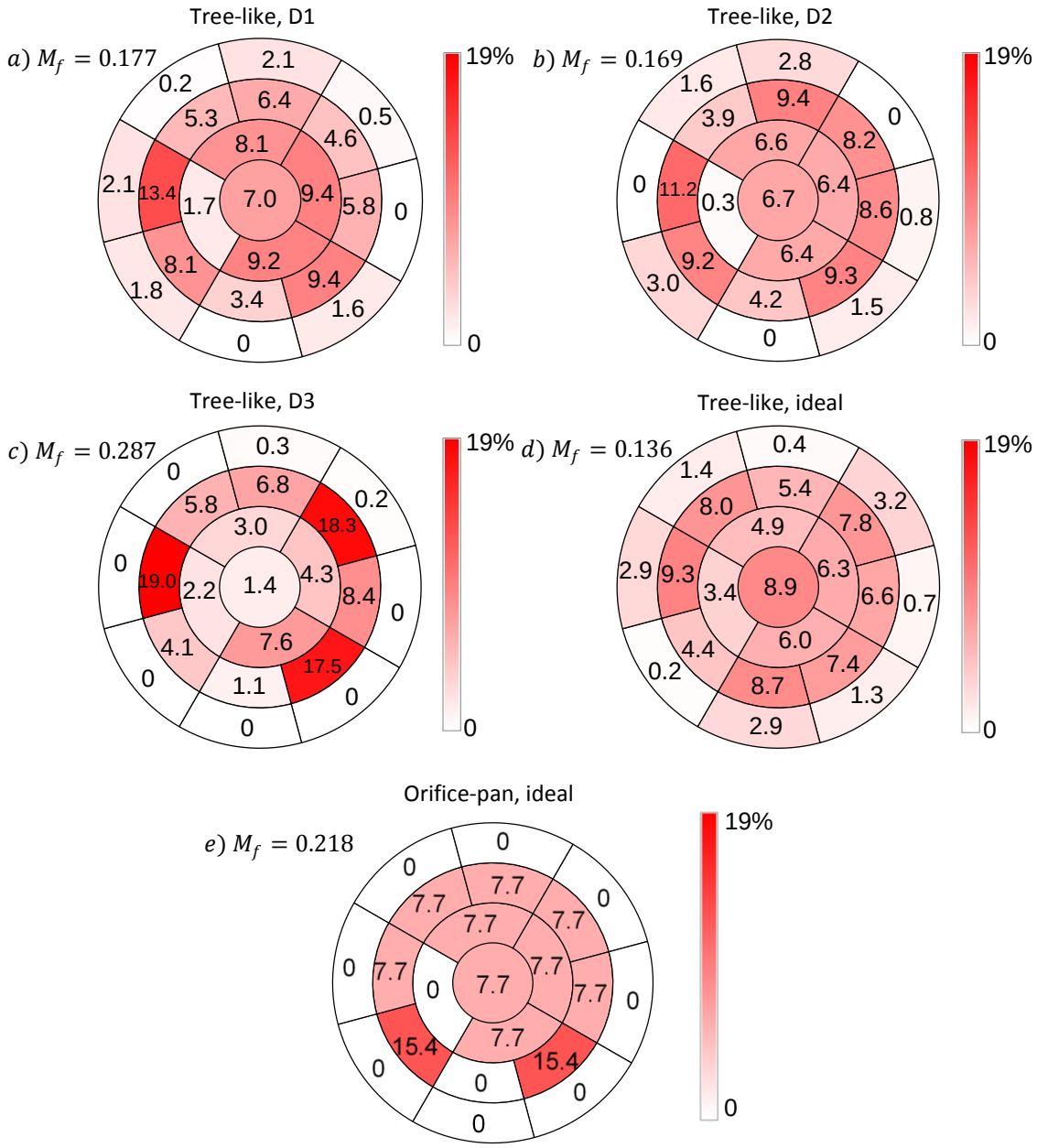

Figure 7 – Experimental fraction of liquid distributed over the cross-section of the column for different distributors at liquid flowrate of 22.6 $m^3/m^2/h$ (a, b, c), and the ideal theoretical distribution obtained according to Figure 5 for a tree-like distributor (d) and an orifice-pan distributor (e)

This figure shows that the ideal distribution is not homogeneous. As discussed in Section 3.1 and depicted in Figure 5, that happens because the liquid is not evenly distributed over the outlets of the structure, even if the flow splits evenly at every wire intersection. Further, according to Figure 7, distributors D1 and D2 both increase the quality of the liquid distribution when compared to the experimental value of the orifice-pan distributor (M_f = 0.218). However, that is not the case for D3, whose maldistribution factor is worse and whose

spatial distribution is more alike the orifice-pan one. This result is even more surprising due to the fact that D3 was conceived in an attempt to ensure wetting flow regime throughout the structure. A possible reason for the poor liquid distribution provided by D3 is the formation of pronounced liquid menisci on the wire junctions due to the large wire diameters. As visual observations corroborate, this results in the formation of liquid membranes similar to those described in Section 2.2, which create preferential flow paths in the structure.

Such preferential paths obtained for water ($\gamma = 71.7$ mN/m) persist even at lower liquid surface tension values. Experiments with 3.1 wt% ethanol + water ($\gamma = 55.7$ mN/m) and 20.5 wt% ethanol + water ($\gamma = 33.2$ mN/m) resulted in maldistribution factors of 0.312 and 0.289 respectively.

To study the impact of flowrate Q on the quality of the distribution, experiments were also carried using $Q = 300$ L/h (17m^3/m^2/h) and $Q = 500$ L/h (28.3m^3/m^2/h). The results are given in Table 3. For reference, the M_f values for the orifice-pan (13 irrigation points) and the perforated pipe (5 irrigation points) distributors are respectively 0.218 and 0.404.

Table 3 – Maldistribution factors measured at different flowrates

	M_f		
Q (m^3/m^2/h)	D1	D2	D3
17.0	0.228	0.252	0.308
22.6	0.177	0.169	0.287
28.3	0.179	0.197	0.271

The lowest flowrate corresponds to the worst distributions, which is likely due to the dominance of the capillary flow regime mentioned in Section 2.2. This hypothesis is endorsed by the diagram presented in Dejean et al. (2020): at $Q = 300$ L/h (17.0 m^3/m^2/h), all layers of D1, D2 and D3 are deep inside the capillary zone.

3.3 Experimental results for HETP

Experiments to measure HETP were performed according to the procedure described in Section 2.4.2. Five different types of distributors (D1-D3, orifice-pan with 13 irrigation points, and Sulzer's distributor with 5 irrigation points) were compared in a column packed with Pall rings (15mm size). Besides, 3 distributors (D1, Sulzer's and orifice-pan) were

compared in a column with the Tetra Spline (TS) packing described in Section 2.3. Figure 8 shows the results obtained from these tests.

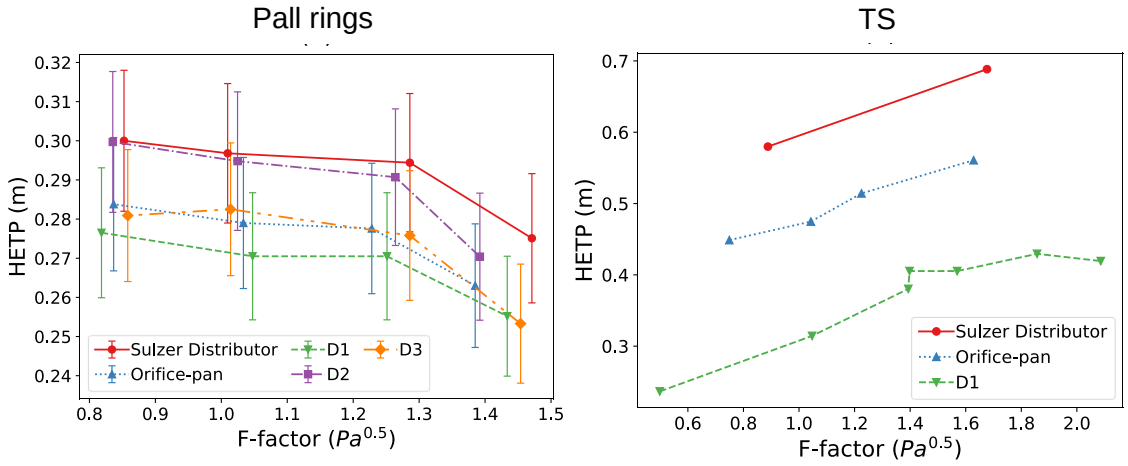

Figure 8 – HETP for 5 different distributors, using Pall rings (left) and TS (right) packings, with the test rig described in Section 2.4.2

The relative error for all HETP measures is estimated around 6%, and it comes from the densitometry accuracy of ± 0.001 g/cm^3 and from deviations in molar fraction in the Wilson activity coefficient model (mean deviation of ±0.0008; maximum deviation of ±0.0025).

The left plot in Figure 8 shows that the efficiency of the Pall rings packing is approximately the same for all liquid distributors. The reason is that the lowest drip point density (283 pts/m^2 for Sulzer's distributor) is already too high. Indeed, it has been shown that densities beyond 100 pts/m^2 do not bring significant improvement in industrial packing efficiency (Kister, 1990; Kister et al., 2008).

Experiments using Mellapak 250Y bed confirm that the tree-like configurations D1-D3 do not decrease HETP of industrial packings. This result does not imply that distribution itself is not improved: as shown in Section 3.2, the maldistribution factor can be decreased from 0.218 up to 0.169 with the addition of the tree structures to an orifice-pan distributor with 13 points. However, such an improvement is not reflected in a better distillation performance when Pall rings or Mellapak 250Y are employed. Other applications possibly more sensitive to liquid maldistribution, such as multiphase reactions and chemical absorption, could benefit from it.

Another important information retrieved from experiments with industrial packings is that mass transfer effects at the distributor level have negligeable impact on HETP results, as these

values remain unaltered by the addition of the tree structures. This result is reasonable, since the height of these structures is only about 0.07 m, which is 7% the height of the packed bed.

However, tree distributors are capable of reducing HETP when coupled with the TS structured packing (Kawas et al., 2021), as illustrated by the right plot in Figure 8. The vertical error bars were omitted from the plot because these errors are small compared to the range of HETP values obtained. TS packing greatly benefits from the tree-shaped distributor, which reduces HETP by up to 50% at low F-factors. The performance of the TS packing depends significantly on the initial distribution, which could be due to the fact that the liquid distribution provided by the packing is itself very dependent on the initial distribution. Figure 9 confirms this hypothesis. In this figure, the liquid distributions are compared for a 1 m packed bed using Sulzer and D1 distributors to provide the initial distribution. The maldistribution factor for the configuration with D1 is less than half of the M_f obtained using Sulzer's distributor with 5 irrigation points.

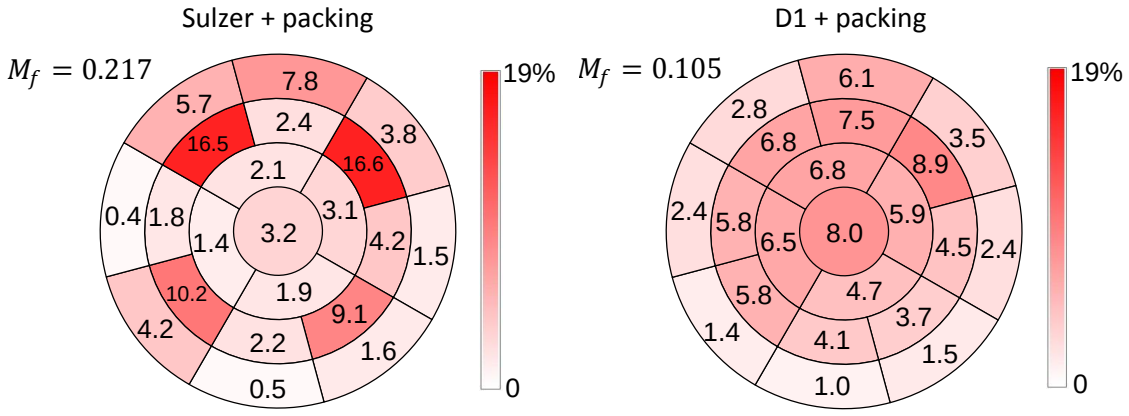

Figure 9 – Liquid repartition at the bottom of a 1 m TS packed bed using Sulzer and D1 distributors for initial distribution

Finally, the pressure drops measured using the TS packing (plots omitted for conciseness) are significantly smaller than those measured using Pall Rings, showing that the former bed has a much lower packing factor. Further, it was found that pressure drop is not affected by the type of liquid distributor when Pall rings packing is employed. This is because the main source of energy loss in this case is friction against the packing. However, for the range of pressure drops found in TS experiments, small variations are observed according to the type of liquid distributor used. The Sulzer distributor increases the pressure drop slightly. In addition, vapor flow obstruction due to the wire structure in D1 is probably the reason for it causing slightly larger pressure drops than the orifice-pan distributor.

The data corresponding to figures 7 to 9 are provided as supplementary material.

4. Conclusion

A new liquid distributor is presented in this paper. It shows that a properly designed tree-like distributor with flow outside the wires reduces maldistribution under several operating conditions whose limits are discussed. The top of the distributor is similar to the regular orifice-pan type, but wires are added below. These wires form a tree structure that guides the liquid dripping from the holes and distributes it over the column's cross-section. Three different tree-like configurations were designed using Autodesk Inventor (2019) and printed in a 3D printer. The design stage involves careful consideration of various geometric and performance constraints. A 4th distributor was printed, which serves as benchmark for comparison with the previous ones. It consists in an orifice-pan distributor with 13 holes.

Theoretical liquid distribution was assessed by using the maldistribution factor M_f. The tree-like distributor invention improves liquid distribution over the column's cross-section. For an ideal 13-holes orifice-pan distributor with $M_f = 0.236$, adding the tree structure with 6 layers can in theory decrease the maldistribution factor up to $M_f = 0.136$. However, M_f measurements remained between 0.169 and 0.308, as depicted in Table 3. At $Q = 300$ L/h, capillary flow regime dominates, and liquid distribution is not improved by the tree structures.

For the industrial packings Pall Rings and Mellapak 250Y, the improvement in initial liquid distribution does not result in better separation efficiency. This result agrees with the empiric rule that drip point densities above 100 pts/m^2 will not improve industrial packing efficiency (Kister, 1990; Kister et al., 2008). Nevertheless, significant improvement in packing efficiency is obtained when tree-like distributors are used along with the TS structured packing disclosed in Kawas et al. (2021). The efficiency of such packing is highly dependent on initial liquid distribution, and the wire structure in the new distributor configuration discussed in Section 2.1 can decrease HETP by 0.18m.

Further experiments using other distributor configurations along with the TS packing could enable finding a quantitative relationship between the quality of the initial distribution and the HETP. Besides, experiments using a smaller number of initial irrigation points and/or larger column diameter could show the impact of this invention on industrial packing efficiency.

Finally, it would be suitable to design and test these new distributors at the industrial scale. For industrial diameters and the same initial drip point density used here (736 pts/m^2), our orifice-pan structure would have much more than 13 drip points. Assuming these drip points are arranged by the designer (design approach), the orifices can be distributed so as to create regular structures such as the one shown in Figure 1c. The distance between drip points distributed in this regular fashion do not scale with the diameter if we keep drip point density constant. For example, the closest drip points in our distributor (made for a column with diameter 0.15 m) were separated by a distance of ~ 0.049 m. An industrial scale distributor with the same drip point density but 2 m diameter would have a separation of ~ 0.056 m if the orifices are distributed uniformly, which corresponds to an increase in separation of only 14%. If we use the exact same structures depicted in Figure 1d for this 2 m column, the 14% increase in the initial distance between orifices would cause dead spaces on the bottom of the distributor. To avoid this (i.e., to have a compact distributor outlet as the one shown in Figure 1c), one can simply add another layer to the pyramid in Figure 1d. From a retrofit perspective, the drip points are already there, and we only install the tree structures. In this case, we might not be able to obtain regular outlet structures as the one shown in Figure 1c. The number of layers can always be adapted to avoid dead (unirrigated) spaces, but increasing it too much might reduce the flowrate per wire on the last layers, and capillarity effects will decrease the quality of the liquid distribution.

Acknowledgement

The authors gratefully acknowledge the financial support of the ADEME (French Environment & Energy Management Agency) and Toulouse Tech Transfer.

References

Autodesk, 2019. Autodesk Inventor.

Bejan, A., Lorente, S., 2004. The constructal law and the thermodynamics of flow systems with configuration. Int. J. Heat Mass Transf. 47, 3203–3214. https://doi.org/10.1016/j.ijheatmasstransfer.2004.02.007

Bessou, V., Rouzineau, D., Prévost, M., Abbé, F., Dumont, C., Maumus, J.P., Meyer, M., 2010. Performance characteristics of a new structured packing. Chem. Eng. Sci. 65, 4855–4865. https://doi.org/10.1016/j.ces.2010.05.029

Cho, K.H., Lee, J., Kim, M.H., Bejan, A., 2010. Vascular design of constructal structures with low flow resistance and nonuniformity. Int. J. Therm. Sci. 49, 2309–2318. https://doi.org/10.1016/j.ijthermalsci.2010.07.009

Dejean, B., Meyer, M., Rouzineau, D., 2020. Design and conception of an innovative packing for separation column—Part I: Hydrodynamic study on wire intersections. Chem. Eng. Res. Des. 160, 11–19. https://doi.org/10.1016/j.cherd.2020.05.006

Eck, T., Kirsten, K., 2019. Liquid Redistributor. 10,357,740 B2.

Franz, U., Geipel, W., 2019. Liquid Distributor of a Process-Technology Column. 10,272,354 B2.

Hanusch, F., Künzler, M., Renner, M., Rehfeldt, S., Klein, H., 2019. Liquid distributor design for random packed columns. Chem. Eng. Res. Des. 147, 689–698. https://doi.org/10.1016/j.cherd.2019.05.035

Hoek, P.J., Wesselingh, J.A., Zuiderweg, F.J., 1986. Small Scale and Large Scale Liquid Maldistribution in Packed Columns. Chem. Eng. Res. Des. 64, 431–449.

Kawas, B., Mizzi, B., Dejean, B., Rouzineau, D., Meyer, M., 2021. Design and conception of an innovative packing for separation column - Part II: Design and characterization of a wire based packing. Chem. Eng. Res. Des. 169, 189–203.

Kister, H.Z., 1990. Distillation Operation. McGraw-Hill, New York.

Kister, H.Z., Mathias, P.M., Steinmeyer, D.E., Penney, W.R., Crocker, B.B., Fair, J.R., 2008. Equipment for Distillation, Gas Absorption, Phase Dispertion, and Phase Separation, in: Green, D.W., Perry, R.H. (Eds.), Perry’s Chemical Engineer’s Handbook. McGraw-Hill, New York.

Komori, T., Ohe, S., 1990. Vapor-liquid-equilibrium data for the system-cyclohexane-n-heptane at atmospheric-pressure. Kagaku Kogaku Ronbunshu 16, 384–387.

Lämmermann, M., Schwieger, W., Freund, H., 2016. Experimental investigation of gas-liquid distribution in periodic open cellular structures as potential catalyst supports. Catal. Today 273, 161–171. https://doi.org/10.1016/j.cattod.2016.02.049

Manteufel, R.P.C., 2000. Super 3X-Pack and Super 4X Pack - A new generation of structured packings.

Manteufel, R.P.C., Koch, J., 2001. Super X-Pack - A New Generation of Structured Packings, in: Separations Technology. AlChE, Reno, pp. 150–156.

Marcandelli, C., Lamine, A.S., Bernard, J.R., Wild, G., 2000. Liquid Distribution in Trickle-Bed Reactor. Oil Gas Sci. Technol. 55, 407–415. https://doi.org/10.2516/ogst:2000029

Moore, F., Rukovena, F., 1987. Liquid and Gas Distribution in Commercial Packed Towers. CPP Ed. Eur. 11–15.

Olujić, Ž., Seibert, A.F., Fair, J.R., 2000. Influence of corrugation geometry on the performance of structured packings: An experimental study. Chem. Eng. Process. Process Intensif. 39, 335–342. https://doi.org/10.1016/S0255-2701(99)00095-1

Olujić, Ž., Seibert, A.F., Kaibel, B., Jansen, H., Rietfort, T., Zich, E., 2003. Performance characteristics of a new high-capacity structured packing Chem. Eng. Process. 42, 55–60. https://doi.org/10.1016/S0255-2701(02)00019-3

Rouzineau, D., Meyer, M., Dejean, B., 2020. Distributeur filaire de liquide pour colonne a garnissage (Patent). FR3113611.

Spiegel, L., 2006. A new method to assess liquid distributor quality. Chem. Eng. Process. Process Intensif. 45, 1011–1017. https://doi.org/10.1016/j.cep.2006.05.003

Subawalla, H., González, J.C., Seibert, A.F., Fair, J.R., 1997. Capacity and Efficiency of Reactive Distillation Bale Packing: Modeling and Experimental Validation. Ind. Eng. Chem. Res. 36, 3821–3832. https://doi.org/10.1021/ie970050l

Wolfram|Alpha, 2020. Wolfram|Alpha [WWW Document]. URL https://www.wolframalpha.com/ (accessed 11.13.20).